17th World Conference on Earthquake Engineering, 17WCEE
Sendai, Japan - September 13th to 18th 2020

THERMAL-MECHANICAL COUPLED ANALYSIS MODEL FOR MATRIX SLIDING BEARINGS

M. Kikuchi[(1)], K. Ishii[(2)], T. Mori[(3)], R. Kurosawa[(4)], H. Sugiyama[(5)], T. Koizumi[(6)]

[(1)] *Professor, Hokkaido University, mkiku@eng.hokudai.ac.jp*
[(2)] *Assistant professor, Hokkaido University, ishii@eng.hokudai.ac.jp*
[(3)] *Senior Researcher, Daiwa House Industry, m269957@daiwahouse.jp*
[(4)] *Managing Director, Kurosawa Construction, r_kurosawa@kurosawakensetu.co.jp*
[(5)] *Deputy Manager, BBM, h-sugiya@mgb.gr.jp*
[(6)] *Manager, BBM, t-koizum@mgb.gr.jp*

Abstract

Seismic isolation is one of the most effective technologies for protecting structures from the damaging effects of earthquakes. Seismic isolation devices lengthen the fundamental period of buildings, diminishing the acceleration response. However, long-period and long-duration ground motions might cause excessive response deformation in the isolation devices. Analyzing the response characteristics for large earthquakes is important to determine the aseismic performance of seismically-isolated buildings. This research focuses on the thermal-mechanical coupled behavior of sliding bearings with multiple sliding units under long-period long-duration ground motions. A sliding bearing comprises a plane sliding plate, a matrix of individual sliding units, and multilayered rubber and steel plates. The hysteretic damping on the sliding surface generates a considerable amount of heat, and deteriorates the friction coefficient of the isolation device.

First, multiple cyclic loading tests were conducted on sliding bearing cutout specimens. The dependencies of the friction coefficient on compressive stress and sliding speed had been determined by other loading test results. By eliminating these two dependencies from the cyclic test results, a dependency of the friction coefficient on contact surface temperature was identified. A numerical hybrid analysis model for the bearings was then proposed. The authors developed the analysis model by combining two models for seismic response analysis and thermal conductivity analysis, respectively. The thermal conductivity analysis model was developed to represent a distributed arrangement of the matrix of sliding units. Using the proposed model, the loading tests were simulated. The results showed a good agreement with the test results and validate the accuracy of the numerical model. After that, a loading test simulation for a real-scale bearing was performed. The results indicated that the increase in temperature on the sliding surface of the real-scale bearing was similar to that of the cutout specimen. Finally, earthquake response analyses of seismically-isolated structures supported by sliding bearings and elastomeric bearings were conducted. Long-period long-duration earthquakes were selected for input ground motions to investigate the response characteristics of severe earthquakes. The results indicated that the heat generation in the sliding surface greatly affected the responses of the isolators. By considering the thermal-mechanical coupled behavior, the response deformation increased because the friction coefficient decreased. For comparison, a simulated sliding bearing model, which has an equivalent single sliding unit, was also used for the response analyses. The area of the single sliding unit of the simulated model was the same as the total area of the matrix of sliding units of the real-scale model. The results indicated that the distributed arrangement of the sliding units decreased the temperature increase on the sliding surface and prevented the deterioration of the friction coefficient.

Keywords: seismic isolation; sliding bearing; thermal conductivity analysis; earthquake response analysis

1. Introduction

Seismic isolation is one of the most effective technologies for protecting structures from the damaging effects of earthquakes. In designing seismic isolation systems, it is most important to make the fundamental period of structures longer than the predominant period of ground motions caused by earthquakes. Seismic isolation devices are horizontally flexible, and they lengthen the fundamental period of buildings, diminishing the acceleration response and structural damage in a superstructure efficiently. Sliding bearings are one of the most common seismic isolators in Japan. These bearings typically consist of an elastic component and sliding component. They can lengthen the fundamental period and also decrease the seismic input energy in superstructures by hysteretic damping.

However, mega-earthquakes from subductions around Japan are a great concern in this research area. Such earthquakes are predicted to cause long-period, long-duration ground motions [1]. Long-period components might resonate with a long-period structure to cause excessive deformation of isolators, and long-duration motions might cause isolators to deform over dozens of cycles. Analyzing the response characteristics for large earthquakes is important to determine the aseismic performance of seismically-isolated buildings. Under severe earthquakes, the hysteretic damping on the sliding surface of the sliding bearings generates a considerable amount of heat, and deteriorates the friction coefficient of the isolation device [2].

This research focuses on the thermal-mechanical coupled behavior of sliding bearings with multiple sliding units under long-period long-duration ground motions. The sliding bearing comprises a plane sliding plate, a matrix of individual sliding units, and multilayered rubber and steel plates [3]. First, multiple cyclic loading tests were conducted on sliding bearing cutout specimens. The dependencies of the friction coefficient on compressive stress and sliding speed had been determined by other loading test results [4]. By eliminating these two dependencies from the cyclic test results, a dependency of the friction coefficient on contact surface temperature was identified. A numerical hybrid analysis model for the bearings was then proposed. The authors developed the analysis model by combining two models for seismic response analysis and thermal conductivity analysis, respectively. The hybrid model is an extension of a previously developed coupled analysis model [5]. The thermal conductivity analysis model was developed to represent a distributed arrangement of the matrix of sliding units. Using the proposed model, the loading tests were simulated. The results showed a good agreement with the test results and validate the accuracy of the numerical model. After that, a loading test simulation for a real-scale bearing was performed. The results indicated that the increase in temperature on the sliding surface of the real-scale bearing was similar to that of the cutout specimen. Finally, earthquake response analyses of seismically-isolated structures supported by sliding bearings and elastomeric bearings were conducted. Long-period long-duration earthquakes were selected for input ground motions to investigate the response characteristics of severe earthquakes. The results indicated that the heat generation in the sliding surface greatly affected the responses of the isolators. By considering the thermal-mechanical coupled behavior, the response deformation increased because the friction coefficient decreased. For comparison, a simulated sliding bearing model, which has an equivalent single sliding unit, was also used for the response analyses. The area of the single sliding unit of the simulated model was the same as the total area of the matrix of sliding units of the real-scale model. The results indicated that the distributed arrangement of the sliding units decreased the temperature increase on the sliding surface and prevented the deterioration of the friction coefficient.

2. Loading tests of cutout specimens

2.1 Matrix sliding bearing

Fig. 1 shows a schematic view of a matrix sliding bearing [3]. The sliding surface consists of a plane sliding plate and a matrix of individual sliding units. The design value of the friction coefficient is 0.032. The rubber bearing part consists of an upper (sole plate side) steel plate, a rubber pad, and a lower (base plate side) steel

plate. The lower plate has a circular opening in the center to improve the bearing's followability to rotational deformation of pile top. Materials used for the matrix bearing are summarized in Table 1.

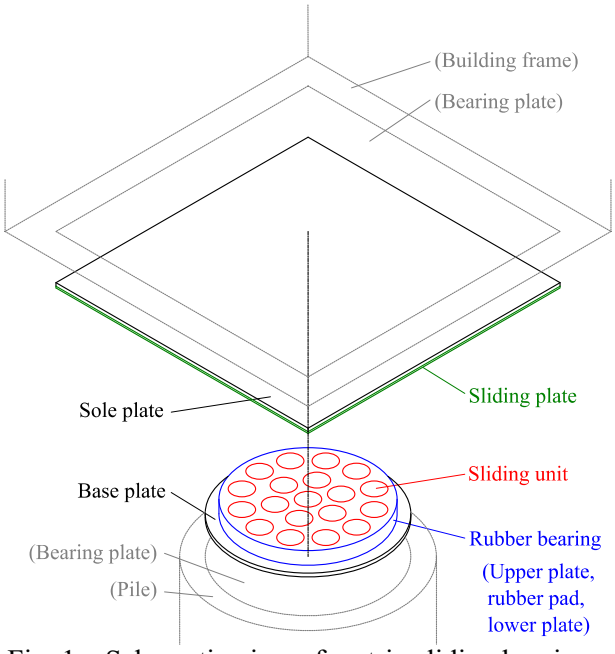

Fig. 1 – Schematic view of matrix sliding bearing

Table 1 – Materials for sliding bearing

SUS	Sliding plate
Polyamide	Sliding unit
Natural rubber (G1.0)	Rubber pad
Steel	Sole plate Base plate Upper/lower plate

2.2 Loading tests

Table 2 and Fig. 2 show the parameters and a design of the cutout specimen for loading tests, respectively. The specimen has a cutout shape of a real-scale device described later in Section 3.2. The bearing consists of seven sliding units and a steel plate. Heat insulation plates with a 10-mm thickness were used under and above the test specimen. The loadings tests were conducted using three cutout specimens and sliding plates.

Table 2 – Test parameters

Axial Load	2200 kN
Peak longitudinal displacement	200 mm
Loading period	4.93 s (sinusoidal)
Number of cycles	50×3

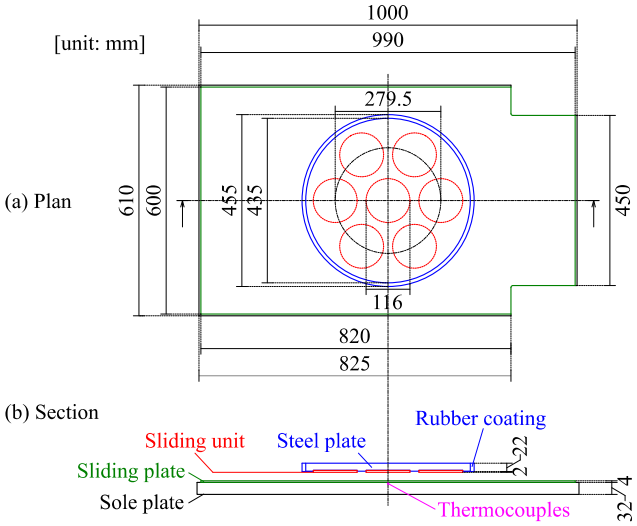

Fig. 2 – Design of cutout specimen for loading tests

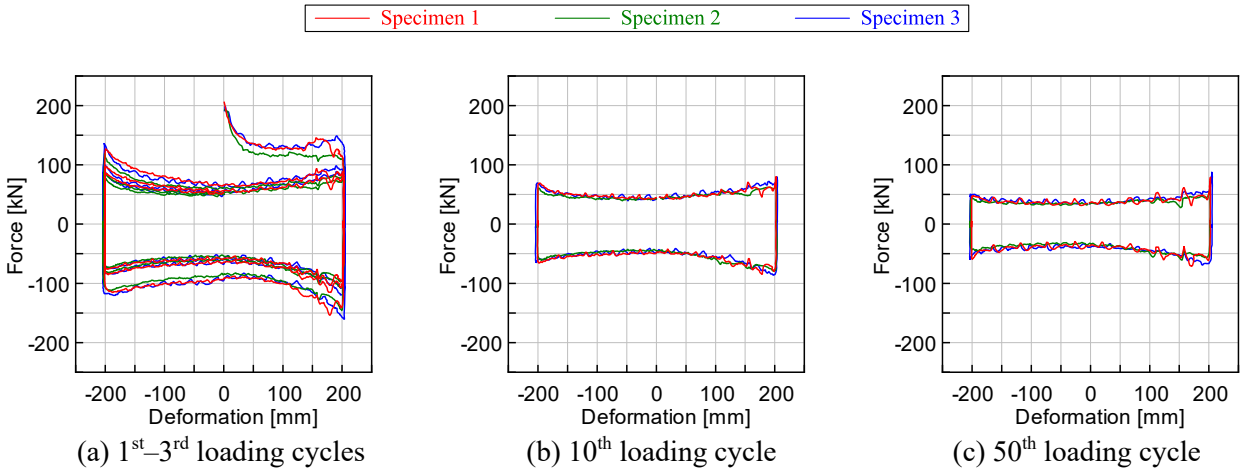

(a) 1st–3rd loading cycles (b) 10th loading cycle (c) 50th loading cycle

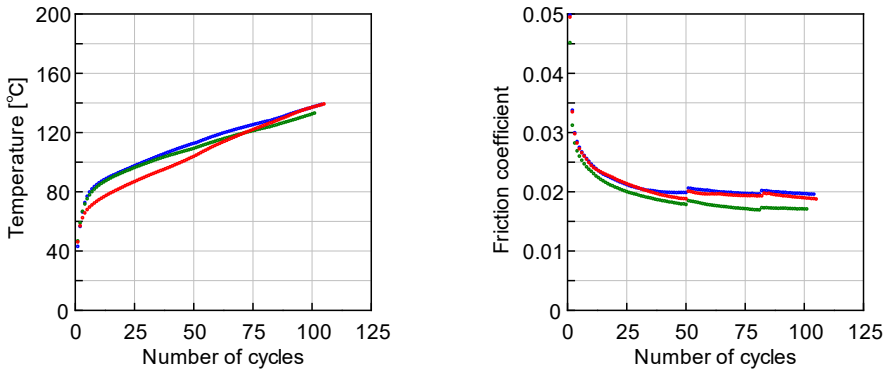

(d) Temperature (e) Friction coefficient

Fig. 3 – Test results for cutout specimens

Figs. 3 (a), (b), and (c) show the force-deformation relationship for the 1st–3rd, 10th, and 50th loading cycles, respectively. The test results of the three specimens are illustrated together. Hysteretic areas diminished during the three loading cycles from the beginning, and almost converged in the 50th cycle. Peak loads were observed at peak deformations. This trend can be accounted for by velocity dependency and temperature dependency of the friction coefficient. Figs. 3 (d) and (e) show the temperature observed at the back center of the sliding plate and the friction coefficient calculated from the hysteretic area, respectively. For these two graphs, the test results after the 51st loading cycle are joined to obtain a consecutive temperature rise. The temperature continued to increase with subsequent loading cycles, but the friction coefficient converged to a lower bound value.

2.3 Evaluation of the friction coefficient

Evaluation formulae for the sliding unit used in the test specimen are identified from experimental results using the same sliding bearings [4]. The standard friction coefficient, μ_0, dependency on vertical pressure, σ [MPa], and dependency on sliding velocity, v [mm/s], can be expressed as Eqs. (1) to (3):

$$\mu_0 = 0.0316 \tag{1}$$

$$\mu_\sigma = 0.231\sigma^{-0.742} + 0.000629 \tag{2}$$

$$\mu_v = -0.0112\ln[\max(v,10)] + 0.0987 \tag{3}$$

where μ_0 is the friction coefficient under standard pressure (15 MPa) and standard velocity (200 mm/s). The pressure is calculated as an axial load divided by the area of the sole plate side steel plate. Using Eq. (3), the friction coefficient obtained from the test results in Section 2.2 were corrected to the standard condition by multiplying 0.862 (= $\mu_{v:400}$ / $\mu_{v:255}$). Fig. 4 and Eq. (4) show the relationship between the corrected friction coefficient and the temperature, T [°C].

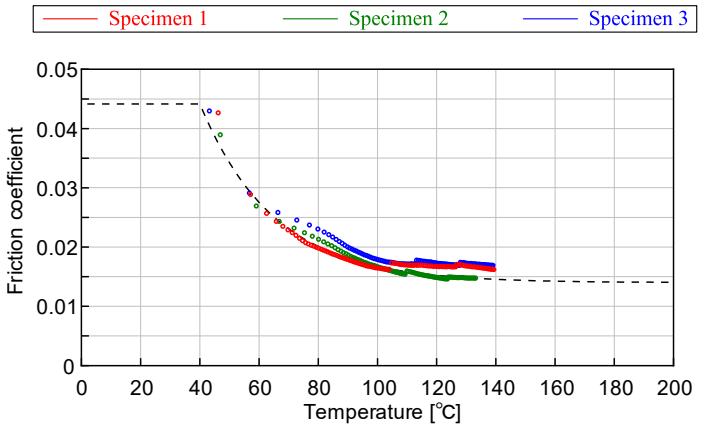

Fig. 4 – Friction coefficient vs. temperature (corrected to standard condition)

$$\mu_T = 0.045\exp[-0.04(\max(T,40) - 30)] + 0.014 \tag{4}$$

3. Simulation analyses of loading tests

3.1 Analysis model

To simulate the mechanical behavior of the matrix sliding bearings under cyclic loadings, an analysis model was developed. This model is an extension of previously developed model [5] and is a combination of a mechanical model and a thermal conductivity model.

Fig. 5 shows an outline of the mechanical model, which consists of a spring element and sliding element in series. Both elements are defined in horizontal 2D plane. An imaginary vertical spring is used to consider the axial load imposed on the bearing.

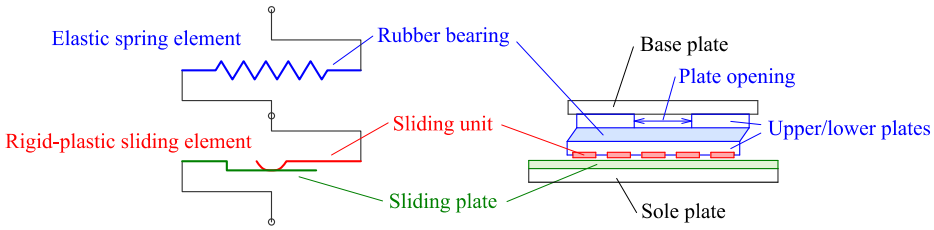

Fig. 5 – Mechanical model for matrix sliding bearing

Stiffness for the elastic element, k, is calculated from Eq. (5):

$$k = \beta GA / t \tag{5}$$

where G is shear modulus of the rubber pad, A is the area of the base plate side steel plate, and t is the thickness of the rubber pad. The effect of the plate opening is considered by coefficient β, with the value of 0.55. The friction coefficient of the sliding element, μ, is calculated from Eqs. (6) to (10), on the basis of the loading test results described in Section 2.3:

$$\mu = (\mu_\sigma / \mu_0) \cdot (\mu_v / \mu_0) \cdot (\mu_T / \mu_0) \cdot \mu_0 \tag{6}$$

$$\mu_0 = 0.0316 \tag{7}$$

$$\mu_\sigma = 0.231\,\sigma^{-0.742} + 0.000629 \tag{8}$$

$$\mu_v = -0.0112 \ln[\max(v,100)] + 0.0987 \tag{9}$$

$$\mu_T = 0.045 \exp[-0.04(\max(T,50) - 40)] + 0.014 \tag{10}$$

where σ [MPa] is the compressive load divided by the area of the sole plate side steel plate, v [mm/s] is the average sliding speed in 0.1 s, and T [°C] is the maximum temperature on the sliding plate surface contacting with the sliding units. To combine all the dependencies of the friction coefficient, the lower bound value for v is modified to separate the low speed effect and low temperature effect. The standard value for T is modified to use the sliding surface temperature.

Fig. 6 shows the thermal conductivity model developed to represent a distributed arrangement of the matrix of sliding units. A 3D difference model is applied to the sliding plate and the sole plate. The cells on the surface of the sliding plate generate/dissipate heat in relation to the displacement of the distributed sliding units.

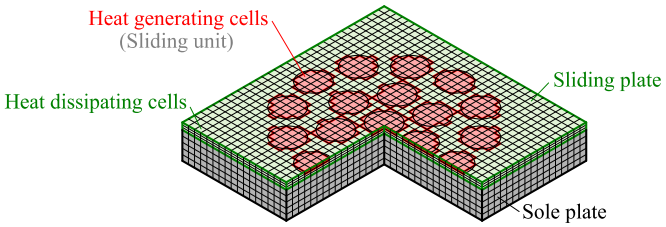

Fig. 6 – Thermal conductivity model for matrix sliding bearing

Distributed energy amount into the heat generating cells was set to 80% of the hysteretic energy calculated from the mechanical model. This correction enables to consider heat dissipation to the sliding units and the rubber bearing indirectly.

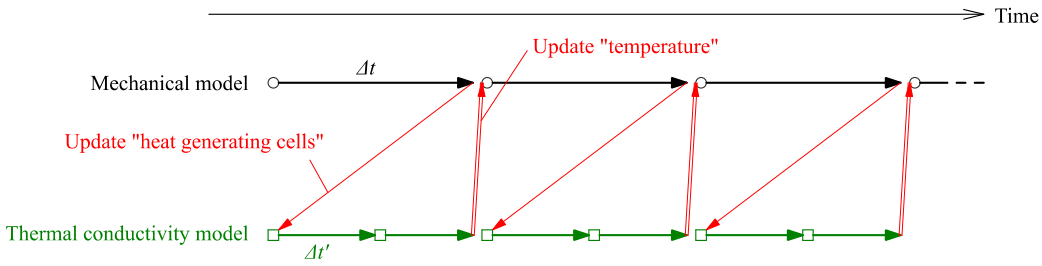

Fig. 7 – Procedure of thermal-mechanical coupled analysis

Fig. 7 shows an outline of combining the two analysis models. This hybrid analysis updates the mechanical model and the thermal conductivity model alternately to reproduce the thermal-mechanical coupled behavior of the bearing. For the mechanical analysis, the Newmark-β method was applied for numerical integration, and time increment, Δt, was set to 0.01 s. For the thermal conductivity analysis, an explicit method was applied, and time increment, Δt', was set to 0.005 s. The developed hybrid analysis model was implemented in OpenSees [6].

3.2 Simulation analyses

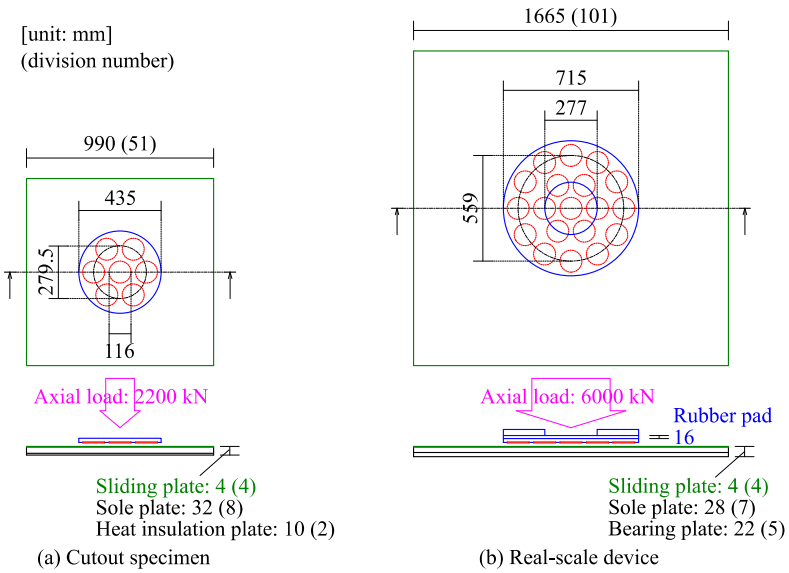

Fig. 8 – Matrix sliding bearing models for simulation analyses

Table 3 – Material constants for thermal conductivity analysis

Material	**Volumetric specific heat [J/(m³·K)]**	**Thermal conductivity [W/(m·K)]**
SUS	3.97×10^6	16
Steel	3.72×10^6	59
Heat insulator	2×10^6	0.4

Fig. 8 shows the analysis models for the cutout specimen used in the loading tests and a real-scale device. A heat insulation plate and a bearing plate are considered in the models to reproduce a realistic configuration. Material constants are summarized in Table 3. On the surface of the sliding plate, the heat transfer coefficient was 25 W/(m²·K). The initial temperature for the thermal conductivity model was 30°C. Sinusoidal loading with a deformation amplitude of 200 mm, a period of 4.93 s, and a cycle number of 125 was applied to the analysis model.

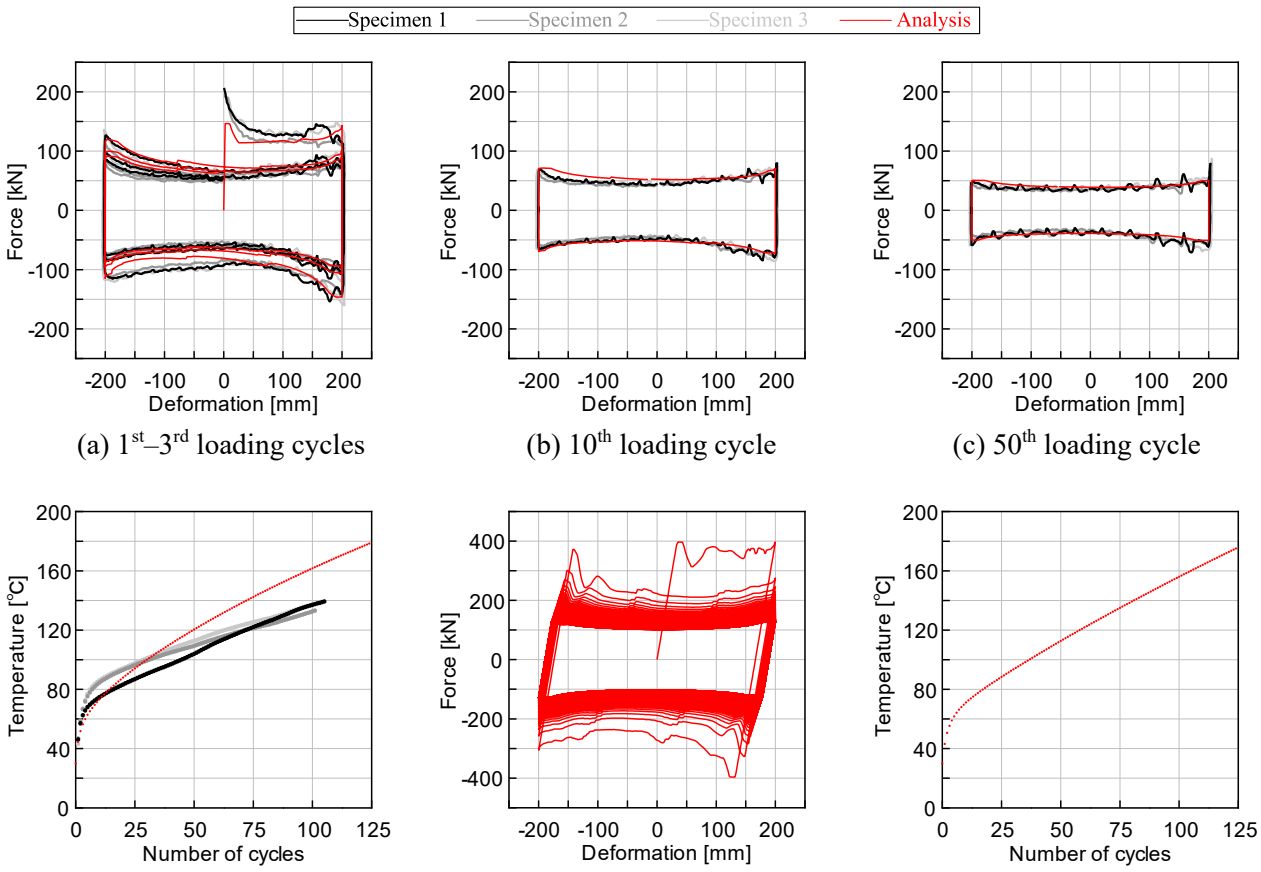

(a) 1st–3rd loading cycles (b) 10th loading cycle (c) 50th loading cycle

(d) Temperature (e) 1st–125th loading cycles (f) Temperature

Fig. 9 – Simulation analysis results (a–d: cutout specimen, e–f: real-scale device)

Figs. 9 (a) to (d) are comparisons of the analysis results to the loading test results using the cutout specimens. The analysis results showed a good agreement with the test results. These comparisons validate the accuracy of the hybrid analysis model. Figs. 9 (e) and (f) are simulation analysis results for a real-scale device. At the beginning of loading, stick-slip motion occurred due to deformation of the rubber pad and nonuniform distribution of surface temperature of the sliding plate. The increase in temperature on the sliding plate of the real-scale device was similar to that of the cutout specimen.

4. Earthquake response analyses of a seismically-isolated building

4.1 Large-sized bearing model

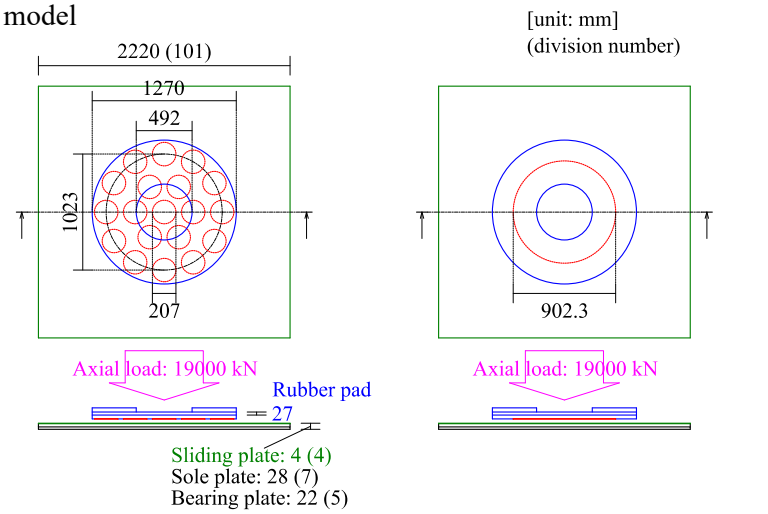

(a) Actual large-sized device (b) Simulated large-sized device (imaginary)

Fig. 10 – Large-sized models for response analyses

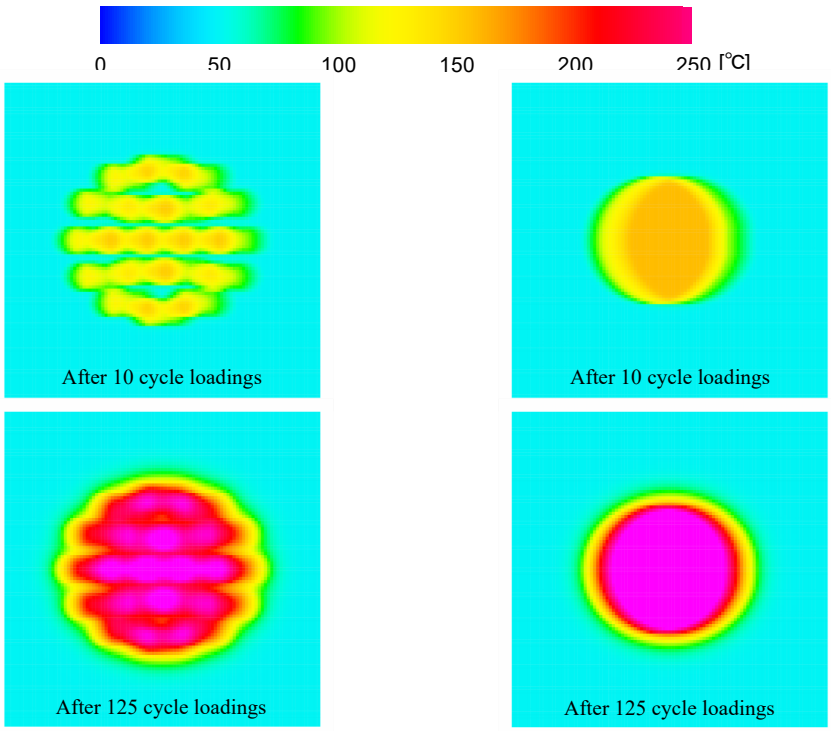

(a) Actual large-sized device (b) Simulated large-sized device

Fig. 11 – Comparison of temperature distribution under cyclic loadings

Fig. 10 shows large-sized bearing models for earthquake response analyses. One is the actual largest bearing with nineteen sliding units, and the other is a simulated model that has an equivalent single sliding unit. The area of the single sliding unit of the simulated device was the same as the total area of the matrix of sliding unit of the actual device. In advance of earthquake response analyses, simulation analyses under cyclic loading were conducted to show the difference between the two large-sized models. Input deformations for the large-sized models are the same as those in the simulation analyses conducted in Section 3.2. Fig. 11 shows the temperature distribution on the surface of the sliding plate. The temperature rise calculated from the actual large-sized device was similar to the analysis result of the real-scale device. On the other hand, the temperature rise in the simulated large-sized device was much higher than that of the actual device. These results indicate that the distributed arrangement of the sliding units decreased the temperature increase on the sliding surface.

4.2 Earthquake response analyses

Fig. 12 shows the input ground motion provided by MLIT in Japan [1]. It had been developed for the purpose of reviewing the design of long-period structures against huge subduction earthquakes. The location of this developed ground motion, OS2, is Osaka city.

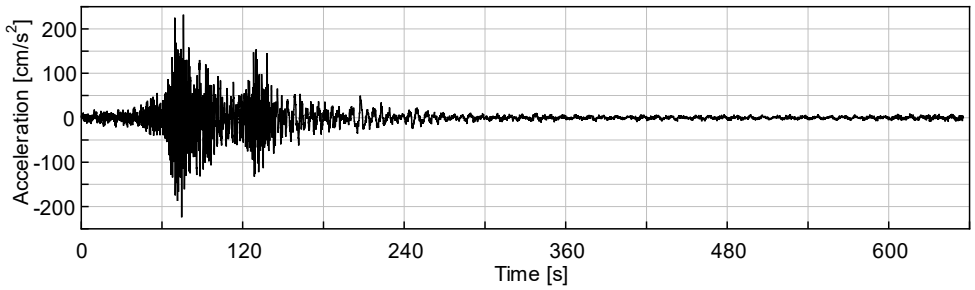

Fig. 12 – Input ground motion, OS2

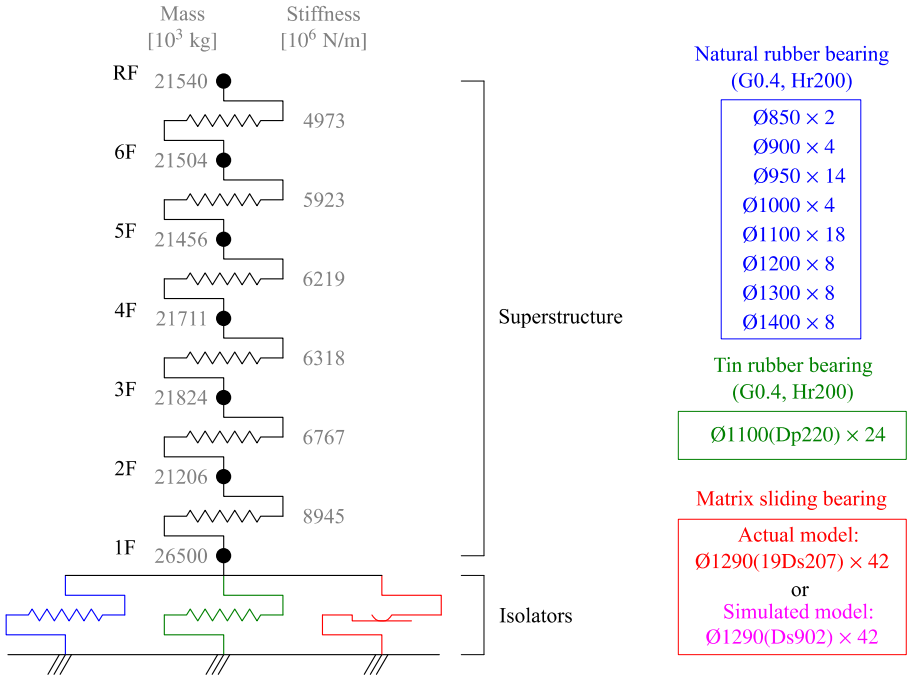

Fig. 13 – Earthquake response analysis model

Fig. 13 shows an earthquake response analysis model for seismically-isolated structures supported by sliding bearings and elastomeric bearings. Elastic linear springs were applied to the superstructure. The fundamental period was 0.725 s when the base of the superstructure was fixed. Stiffness proportional damping was applied to the superstructure with a damping ratio of 2%. Three kind of isolators were used in the model. Natural rubber bearings were modelled as elastic linear springs. Tin rubber bearings were modelled as those from a previously proposed hybrid analysis model [7]. In this research, the yield stress of tin plug, τ_p [MPa], is defined as Eq (11):

$$\tau_p = 25 - 0.218T + 0.000695T^2 \text{ (for } T < 100\text{)}, (230 - \text{T})/12.7 \text{ (for } T \geqq 100\text{)} \quad (11)$$

where T [°C] is the temperature of the tin plug. The two large-sized sliding bearings models were applied to this building model. The sliding plate size was modified with a side length of 2620 mm and a thickness of 5 mm. The initial temperature was set to 20°C for all models.

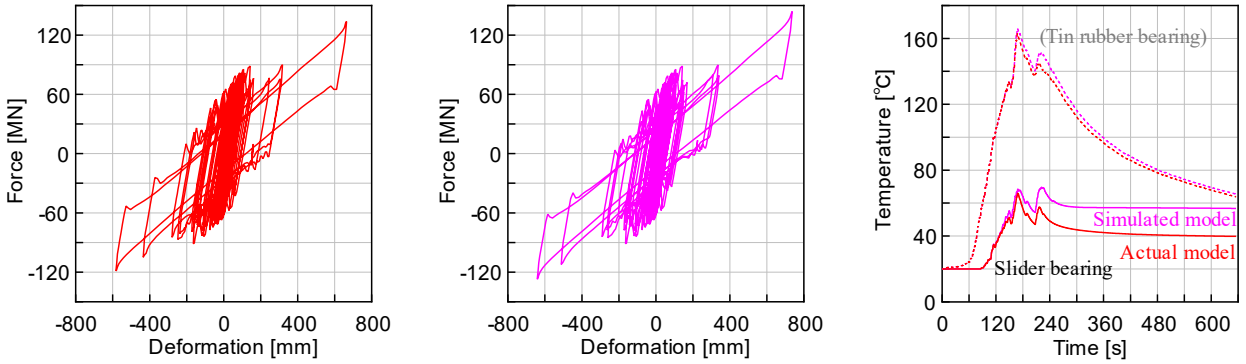

Fig. 14 – Comparison of earthquake response analysis results

Figs. 14 (a) and (b) show the force-deformation relationships of the total number of isolators. The peak deformation in the actual model decreased by 10% compared with that of the simulated model. Fig. 14 (c) shows the comparisons of temperature rises for the isolator models. Distributed arrangement of the sliding units in the actual model prevented a temperature rise and deterioration of the friction coefficient in the sliding bearing, and also decreased the maximum temperature of tin rubber bearing by 10°C indirectly. These results indicate that the heat generation in the sliding surface greatly affected the seismic responses of the isolators.

5. Conclusion

This research focused on the thermal-mechanical coupled behavior of sliding bearings with multiple sliding units under long-period long-duration ground motions. The bearing comprises a plane sliding plate, a matrix of individual sliding units, and multilayered rubber and steel plates. The hysteretic damping on the sliding surface generates a considerable amount of heat, and deteriorate the friction coefficient of the isolation device.

First, multiple cyclic loading tests were conducted on sliding bearing cutout specimens. A dependency of the friction coefficient on the contact surface temperature was identified by eliminating two dependencies on compressive stress and sliding speed.

Next, a numerical hybrid analysis model for the bearings was proposed. A mechanical model and thermal conductivity model were combined to perform thermal-mechanical coupled analysis. Using the proposed model, the loading tests were simulated. Simulation analysis results showed a good agreement with

the test results and validated the accuracy of the numerical model. After that, a loading test simulation for a real-scale bearing was performed. The results indicated that the increase in temperature on the sliding surface of the real-scale bearing was similar to that of the cutout specimen.

Finally, earthquake response analyses of seismically-isolated structures were conducted. For comparison, a simulated sliding bearing model, which has an equivalent single sliding unit, was also used for the response analyses. A long-period long-duration earthquake, OS2, was selected for the input ground motions. The results indicated that the distributed arrangement of the sliding units decreased the temperature increase on the sliding surface and prevented the deterioration of the friction coefficient.

6. Acknowledgements

This research was supported by JSPS KAKENHI Grant Numbers 19H00788 and 19K23546. Dr. Frank McKenna of the University of California, Berkeley, assisted in the implementation of the numerical analysis model in the OpenSees program. The authors would like to express their gratitude for all of the financial support and assistance.

7. References

[1] MLIT (Ministry of Land, Infrastructure, Transport and Tourism, Japan). Homepage, http://www.mlit.go.jp/report/press/house05_hh_000620.html (in Japanese, accessed on January 15th, 2020.)

[2] H. Hibino, R. Maseki, A. Nii, S. Minewaki, M. Yamamoto, H. Yoneda, M. Takayama, M. Kikuchi, M. Iiba. Safety Verification of Seismic Isolation System using Sliding Bearings against Long Period Earthquake Motions. *15th World Conference of Earthquake Engineering*, Lisbon, Portugal, 2012, No. 1377.

[3] T. Mori, C. Sudoh, K. Tanaka, K. Hirai. Experimental study on elastic slide bearing with large rotation capacity (in Japanese). *Summaries of Technical Papers of Annual Meeting*, AIJ, 2016, B-2, No. 21215, pp. 429-430.

[4] BBM. Technical report of DKB elastic sliding bearing (in Japanese), 2015.

[5] K. Ishii, M. Kikuchi. Mechanical behavior of sliding bearings for seismic isolation under cyclic loading. *16th World Conference on Seismic Isolation, Energy Dissipation and Active Vibration Control of Structures*, St. Petersburg, Russia, 2019, pp. 1-10 (in print).

[6] Open System for Earthquake Engineering Simulation – Home Page, http://opensees.berkeley.edu (accessed on January 15th, 2020.)

[7] M. Kikuchi, K. Ishii. Thermal-mechanical coupled behavior of elastomeric isolation bearings under cyclic loadings. *16th European Conference on Earthquake Engineering*, Thessaloniki, Greece, 2018, No. 11240.

